Determination of the structure factor of simple liquid metals from the pseudopotential theory and optimized random-phase approximation: Application to Al and Ga

J. L. Bretonnet
Laboratoire de Physique des Milieux Condensés, Université de Metz, 57045 Metz, France

C. Regnaut
Physique des Liquides et Electrochimie, GR4, Centre National de la Recherche Scientifique, 4 place Jussieu, 75230 Paris, France

(Received 26 April 1984)

We present the results of calculations of the static structure factor $S(q)$ of liquid Al and Ga at the melting point. These calculations were motivated because many simple liquid metals exhibit structure anomalies taking the form of a shoulder on the main peak or even an asymmetry in the peak itself, while other liquid metals are correctly predicted by the standard models of liquid structure. Al and Ga have similar valence, electronic density, and size of their ionic radius; therefore, their pair potentials are somewhat similar. Despite this, their structure factors display most of the differences that can be observed among the variety of liquid metals. Starting from the Shaw optimized model potential [Phys. Rev. **174**, 769 (1968)], a pair potential is constructed. A comparative examination of the electron-gas response function of Vashishta and Singwi [Phys. Rev. B **6**, 875 (1972)] and of Ichimaru and Utsumi [Phys. Rev. B **24**, 7385 (1981)] is carried out. Different depletion hole distributions are also used and full nonlocality is taken into account through effective masses. So $S(q)$ is calculated by means of the optimized random-phase approximation. Particular attention is also devoted to the low-q region. By comparison with Monte Carlo computation, we show the limitation of various thermodynamic perturbation methods, such as the random-phase approximation or the soft-sphere model. The study of $S(q)$ provides a stringent test of the model potential, where the electron-ion pseudopotential and the local-field correction are of prime importance, but where effective masses and depletion hole distribution may also have a role to play.

I. INTRODUCTION

It is well known that the hard-sphere fluid provides us with a crude but successful model of the liquid-metal structure factor (Ashcroft and Lekner[1] and Waseda[2]). However, the numerous experimental and theoretical studies concerning this quantity indeed show that the accurate determination of the interactions which lead to the liquid-metal structure is a difficult task that is far from being achieved. A survey of some recent papers (Regnaut *et al.*,[3] Beck and Oberlé,[4] Evans and Sluckin,[5] Rami Reddy *et al.*,[6] McLaughlin and Young,[7] Kahl and Hafner,[8] and Bretonnet *et al.*,[9]) suggests that further progress is possible, provided that we bear in mind at least three points:

(i) The very careful measurement[10] of the structure factor $S(q)$ at low wave number q. With no such accurate data we can only speculate on the theoretical low-q behavior.

(ii) The determination of the effective interionic interactions in the metal by means of the nonlocal pseudopotential formalism (e.g., the optimized model potential). It is well established that the effective pair potential of the liquid metals has a long-range oscillatory tail. A local pseudopotential approach, used to calculate this tail as well as its associated properties, is often too crude.

(iii) The application of improved thermodynamic perturbation theories to the liquid metals appropriate to the long-range nature of the interionic interactions. For this purpose the so-called optimized random-phase approximation (ORPA) and optimized cluster theory (OCT) are promising approaches. We know, of course, that accurate results may be obtained directly by computer simulation of the liquid state, but in the case of the long-range pair potentials large samples are required, and, thus, calculations may be done at the expense of long computation time. Therefore, any practical study involving the systematic calculation of several properties at various temperatures and densities may first be undertaken by means of a suitable analytical method.

We must point out that the three preceding points are, in fact, connected. If we dispose of accurate $S(q)$ data at low q, we must, in turn, improve both the theoretical approach of the effective interionic pair potential $v(R)$ at large distances and the thermodynamic perturbation theory which links $v(R)$ to $S(q)$.

The aim of this paper is to determine the simple liquid-metal structure factors according to the above arguments. Nevertheless, our results will focus on polyvalent metals rather than alkali metals. The latter have been quite extensively described in the literature, and, moreover, they are less sensitive than polyvalents to the various approximations of the pseudopotential and thermodynamic perturbation methods. Here we illustrate our

calculations with aluminum and gallium. These two simple metals are similar if we consider their valence, electronic density, and the size of their ionic radius. Therefore, their effective interionic pair potentials are somewhat similar. Despite this, Al and Ga liquid structure factors exhibit most of the differences that will be observed among the variety of liquid metals. Thus the study of these two metals provides a stringent test of the pseudopotentials.

Our work is arranged as follows. Firstly, we summarize the main differences between the hard-sphere-fluid model and the liquid-metal structure factor, and we point out some of the recent results of the literature. Secondly, we present the pair potentials derived from the Shaw[11] optimized model potential. Similar pair-potential calculations were carried out earlier by Kumaravadivel and Evans[12]. However, since our structure calculations point out the importance of long-range interactions, we must perform further analyses of the various approximations which enter into the pair-potential derivation. Thus, even with a well-established model like the optimized Shaw model, we must work with a class of pair potentials, corresponding to a series of well-defined approximations, otherwise the discussion of results with only some potentials taken at random may indeed mask the inherent limitations of standard pseudopotential theory. Thirdly, we discuss the ORPA scheme in order to derive structure factors, and we give a detailed analysis of the low-q region. Finally, we compare the aluminum and gallium structure factors as predicted by the optimized model to the experimental data.

II. SURVEY OF THE LIQUID-METAL STRUCTURE FACTOR

The differences between the liquid-metal- and hard-sphere-model structure factors are more or less pronounced. They depend on the investigated metal and the explored range of q. In order to characterize such differences we find it convenient to distinguish three regions in q space, labeled I, II, and III. Region I corresponds to the large-q region, i.e., beyond the second oscillation of $S(q)$. Region II involves the main peak of $S(q)$ and corresponds to wave number $q_p \simeq 2\pi/\sigma$ (σ is the hard-sphere diameter of the reference system). Region III is the low-q region.

The main disparities between the observed $S(q)$ and the hard-sphere-fluid model in region I concern the position of the oscillations and their decay. In the model they may be shifted towards high q and their decay is less pronounced. This feature is quite well observed in the case of alkali metals.

In region II the hard-sphere model is often successful in reproducing the $S(q)$ profile, although it is difficult to fit the height and position of the experimental main peak exactly. Moreover, in some cases the $S(q)$ profile is not at all hard-sphere-like. It is well known that the $S(q)$ first peak is asymmetric (e.g., Zn, Cd, or Hg) or nonmonotonic. For instance, Ga, Sn, and Bi structure factors have a pronounced shoulder to the right of the main peak.

In region III the discrepancy between the measurements and the hard-sphere model is chiefly characterized by the limit $S(q=0)$. This quantity may be obtained experimentally, either by an extrapolation of the low-q structure-factor data or from the isothermal compressibility by using the result of fluctuations of macroscopic density, $S(0)=nk_BT\chi_T$. Near the melting point the standard hard-sphere model of Ashcroft and Lekner[1] leads to $S(0)\simeq 0.025$. This value is close to the experiments on alkali metals.[13,14] Some polyvalent metals, such as Mg, truly agree with the standard value of 0.025; in return, considerable deviation is observed for Sn (0.007) and Ga (0.005).

One analysis of the discrepancies between the hard-sphere model and the observed $S(q)$ has been proposed for region I by Jacobs and Andersen.[15] These authors obtain a satisfactory explanation of the larger-q behavior of $S(q)$, assuming that the interaction potential is soft at short range. This assumption applies to the polyvalent metals, but in the case of alkali metals, which have presumably softer cores, the soft-sphere thermodynamic perturbation method is less convenient[7] and may be replaced by a simulation method such as that realized earlier by Day *et al.*[16]

The discrepancies concerning region II have been studied on the basis of numerous models. At normal liquid densities the structure factor at intermediate and large q is mainly determined by the short-range repulsive potential, but, if the remaining part of the pair potential has spatial variations such as those ascribable to pseudopotential theory, then this part of the potential also contributes to the structure. For instance, some peculiarities of the $S(q)$ profile may be attributed to the Friedel oscillations.[17–20] Asymmetry, or the shoulder or the main-peak profile, arises when the oscillatory tail of the potential exhibits appreciable Fourier components near $q_p \simeq 2\pi/\sigma$. However, an interionic potential with a repulsive ledge[21,22] may also produce the particular $S(q)$ profile in region II. The weakness of such an approach lies in the *ad hoc* choice of the potential. We must also mention that the influence of the core polarization on the $S(q)$ profile near $q \simeq q_p$ found by Mon *et al.*[23] has been largely overestimated.

The study of region III undoubtedly causes most of the difficulties. To our knowledge, the first attempt to connect $S(q=0)$ with pseudopotentials was made by Evans and Schirmacher[24] using several thermodynamic perturbation theories, such as the soft-sphere approach of Weeks *et al.*,[25] the random-phase approximation (RPA), and their own extended random-phase approximation (ERPA). More recently, Evans and Sluckin[5] have discussed the choice of the reference system: hard-sphere fluid or one-component plasma (OCP). These authors applied to RPA to the OCP and found it quite accurate to describe the small-q region for the alkali metals, provided the density is not too low. In alkali metals the interionic potential is effectively much softer than in the polyvalent metals, and hence, as a reference system, the OCP is somewhat better than the hard-sphere fluid. On the other hand, the variational approach[26] suggests that the hard-sphere system is superior to the OCP model for Al, contrary to the case for Na.

In their work, McLaughlin and Young[7] compare the $S(q=0)$ values in the following three ways: soft sphere,

RPA, and "mean-density approximation" (MDA). The MDA of Henderson and Ashcroft[27] was thought, by them, to be essentially exact for $0<q<0.4k_F$ (k_F is the Fermi wave number). McLaughlin and Young performed the calculations for Na, Pb, Al, and Mg. Although some failure of the MDA formalism occurs at low q for Pb, the authors concluded that there is a good degree of agreement between theory and experiment for the other three metals. They also emphasized two points in their work. Firstly, the calculated $S(q)$ was found to be sensitive to the Ashcroft core-radius model potential used to derive the pair potential. Secondly, in order to test the liquid interionic potential, it is important to consider the entire structure factor rather than any restricted part of it.

This short review of various attempts to connect pseudopotentials with liquid-metal structure is a good indicator of the need for both improved pseudopotential and thermodynamic perturbation methods. It is generally recognized that Ashcroft's model is a good local model involving only one core-radius parameter. However, all the physical contents of the pseudopotential theory may not emerge through a single empirical fit of this parameter. Here we choose to work with the nonlocal Shaw model. It produces the smoothest pseudo wave function, in the spirit of Cohen and Heine,[28] and provides a unique method for obtaining the optimum core parameters. Among thermodynamic perturbation methods, the ORPA approach is one of the possibilities. Clearly, it is more powerful than others like (i) the soft-sphere method, in which the long-range interactions are neglected, (ii) the RPA, which leads to unphysical pair-correlation function inside the hard core, and (iii) the ERPA and MDA, which are restricted to low q. Moreover, the critical evaluation of the MSA, ORPA, and OCT for the square-well fluid[8] demonstrates that the compressibility, or $S(q=0)$, is equally satisfied by the ORPA and OCT, which both surpass the MSA.

III. EFFECTIVE PAIR POTENTIALS

In the standard pseudopotential theory,[29] the second-order expansion leads to an effective interionic pair potential $v(R)$, which is the sum of the direct ion-ion interaction and an indirect ion-electron-ion interaction,

$$v(R)=\frac{(Z^*)^2}{R}\left[1-\frac{2}{\pi}\int_0^\infty F_N(q)\frac{\sin(qR)}{q}dq\right]. \quad (1)$$

The effective valence of the ions Z^* and the normalized energy wave-number characteristic $F_N(q)$ are well-known ingredients of the theory. From the usual local approach, using, for instance, Ashcroft's empty-core model, Z^* is reduced to the chemical valence, and $F_N(q)$ has a simple expression. The nonlocal derivation of $F_N(q)$ from Shaw's model is much more tedious. Since our work involves short- and long-range pair potentials, we must carefully analyze various factors and approximations leading to $F_N(q)$, as well as their influence on the pair potential.

The basis of Shaw's model is the electron-ion interaction defined by

$$w(r)=-\frac{Z}{r}-\sum_{l=0}^{l_0}\Theta(R_l-r)(A_l-Z/r)P_l\ , \quad (2)$$

where P_l is the projector on the lth angular momentum. The well depths A_l and the radii R_l are related by the optimization condition

$$R_l(E)A_l(E)=Z\ . \quad (3)$$

Here we use atomic units $\hbar=m=e=1$. Although Shaw's model implies a unique set of well depths A_l, their values depend somewhat on the calculation procedure of the required A_l at energy E in the liquid metal. This is one incertitude which appears in the theory, but there are two other basic uncertainties at the second-order perturbation-expansion level. These come from the particular exchange-correlation corrections and the spatial depletion hole distribution. The latter is arbitrary, but we must hope that the results will not be very sensitive to a particular choice for this distribution.

Here, $F_N(q)$ is constructed in the following manner: (i) we first neglect both exchange and correlation as well as effective-mass contributions; (ii) we then correct the previous results by means of a constant-mass approximation; (iii) we finally consider exchange-correlation corrections.

In the first stage, the normalized energy wave-number characteristic is given by[30]

$$F_N(q)=-\left[\frac{q^2}{4\pi\tilde{Z}}\frac{N}{V}\right]^2\left[\frac{1-\epsilon_H(q)}{\epsilon_H(q)}[v(q)+v_d(q)]^2+2g(q)[v(q)+v_d(q)]+\epsilon_H(q)g^2(q)+h(q)\right]. \quad (4)$$

$\epsilon_H(q)$ is the familiar Hartree dielectric function, $v(q)$ is the Coulomb part of the model, $v_d(q)$ is related to the local depletion hole charge, $g(q)$ is the contribution due to the screening of the nonlocal part of the bare-ion model potential, and $h(q)$ also arises from the nonlocal part. In addition, each ion has an effective valence defined by $\tilde{Z}=Z-\rho$. All these quantities have been discussed by Shaw.[30]

The second step includes the modified perturbation theory, which leads to a new expression of the first-order coefficients in the model wave function. This changes both the electronic screening charge and the effective valence and, consequently, the normalized energy wave-number characteristic. Such a modification may be introduced by means of two effective masses.[31] One, which appears as a factor $m_E(k)$ in several quantities, is related to the energy dependence of the model potential $w(r)$ by the relation

$$m_E(k)=1-N\left\langle k\left|\frac{\partial w}{\partial E}\right|k\right\rangle . \tag{5}$$

Simplification involves applying the constant-mass approximation on the Fermi surface, as by Shaw[31]. D'Evelyn and Rice[32] have recently shown that the constant-mass approximation and its treatment leads to insensitive change in the Na pair potential. Here we also assume this for polyvalent metals. The new normalized energy wave-number characteristic is denoted $F_N^*(q)$ and reads

$$F_N^*(q)=\left[\frac{\tilde{Z}}{Z^*}\right]^2\frac{F_N(q)}{m_E^2(k_F)}+\Delta F_N^*(q) , \tag{6}$$

where the new effective mass is $Z^*=Z-\rho/m_E(k_F)$, and the expression for $\Delta F_N^*(q)$ is given by

$$\Delta F_N^*(q)=-\left[\frac{q^2}{4\pi Z^*}\frac{V}{N}\right]^2\left\{\frac{1}{m_E^2(k_F)}\frac{\epsilon_H(q)}{\epsilon^*(q)}\left[\left[\frac{1}{m_E^2(k_F)}-1\right]v_{sc}^2(q)+2v_{sc}(q)v_d(q)\left[\frac{1}{m_E(k_F)}-1\right]\right]\right.$$
$$\left.+\frac{1-\epsilon_H^*(q)}{\epsilon_H^*(q)}v_d^2(q)\left[\frac{1}{m_E(k_F)}-1\right]^2\right\} . \tag{7}$$

$v_{sc}(q)$ corresponds to the potential of the electron screening charge which arises in the usual second-order expansion,

$$v_{sc}(q)=\frac{1-\epsilon_H(q)}{\epsilon_H(q)}[v(q)+v_d(q)]+g(q) . \tag{8}$$

$\epsilon_H^*(q)$ is the renormalized Hartree dielectric function,

$$\epsilon_H^*(q)=1+\frac{1}{m_E^2(k_F)}[\epsilon_H(q)-1] . \tag{9}$$

In the final step, the effects of electron exchange-correlation are included, approximately following the procedure developed by Shaw,[33] so that the normalized energy wave-number characteristic is

$$F_N^{*,xc}(q)=\left[\frac{\tilde{Z}}{Z^*}\right]^2\frac{1}{m_E^2(k_F)}F_N(q)+\Delta F_N^*(q)+\Delta F_N^{xc}(q) , \tag{10}$$

where

$$\Delta F_N^{xc}(q)=\left[\frac{q^2}{4\pi Z^*}\frac{V}{N}\right]^2\frac{\epsilon_H^*(q)}{\epsilon^*(q)}G(q)$$
$$\times\left[\frac{v(q)+v_d(q)}{\epsilon_H(q)}-v(q)+g(q)+\Delta w^*\right]^2 . \tag{11}$$

Δw^* is the correction of the form factor due to the effective mass,

$$\Delta w^*=\left[\frac{1}{m_E(k_F)}-1\right]\frac{1}{\epsilon_H^*}$$
$$\times\left[v_{sc}(q)\left[\frac{1}{m_E(k_F)}+1\right]+v_d(q)\right] . \tag{12}$$

The modified dielectric function $\epsilon^*(q)$ differs from the Hartree result and may be written as

$$\epsilon^*(q)=1+[1-G(q)][\epsilon_H^*(q)-1] . \tag{13}$$

If we wish to carry out only the exchange-correlation corrections, we find that $\Delta F_N^{*,xc}(q)$ can be simplified as in Shaw.[33]

Many forms of the local-field exchange-correlation function $G(q)$ have been suggested in the literature; however, we focus on two. The first comes from Vashishta and Singwi[34] (VS) and is one of the easiest and most accurate forms to handle. The second, recently proposed by Ichimaru and Utsumi[35] (IU), accurately reproduces the Monte Carlo (MC) results on an electron gas and satisfies the self-consistency conditions in the compressibility sum rule and the short-range correlation.

In order to derive $F_N^{*,xc}(q)$, it is necessary to assume a form for the depletion hole distribution. Unfortunately, this function cannot be calculated without knowledge of the conduction-electron wave functions, and it is precisely the intention of model-potential theory to avoid a calculation of these quantities.

In the present work, to get an estimate of the influence of the spatial distribution of the depletion hole, we examine two cases. In the first we submit that all the charge is uniformly spread over a model sphere of radius R_M, which is a weighted mean of the optimized core radius R_l, namely

$$R_M = \frac{\sum_{l=0}^{l_0} (2l+1)R_l}{\sum_{l=0}^{l_0} (2l+1)} , \tag{14}$$

and then

$$v_d(q) = \frac{4\pi}{q^2}\frac{N}{V}\rho M(q) , \tag{15}$$

where

$$M(q) = \frac{3}{qR_M}\left[\frac{\sin(qR_M)}{(qR_M)^2} - \frac{\cos(qR_M)}{qR_M}\right] . \tag{16}$$

The opposite case should be the hole charge localized at the nucleus, i.e., δ-function distribution; however, this is rather unrealistic and leads to $F_N^{*,\mathrm{xc}}(q)$, which is not zero at large q, as it should be. Thus, in the second case, we use the $\exp(-\alpha r)/r$ distribution, which ensures the correct $F_N^{*,\mathrm{xc}}(q)$ asymptotic behavior, leading to

$$M(q) = \alpha^2/(\alpha^2+q^2) . \tag{17}$$

Here, α is chosen in order to obtain 99% of the total depletion charge inside the sphere of radius R_M.

The components of the normalized energy wave-number characteristic being so defined, the only parameters we need for $F_N^{*,\mathrm{xc}}(q)$ are (i) the valence Z, (ii) the Fermi wave number k_F, (iii) the model-potential well depths A_l and their first derivative, $\partial A_l/\partial E$, at the Fermi energy E_F. The calculation of the well depths in the liquid at the observed temperature and density may then be done, once the Fermi level in the liquid band structure has been scaled. The Fermi energy is derived using the Ballentine-Gupta[36] formula for the core shift and the Ese-Reissland[37] procedure. Density versus temperature dependence is taken from Crawley.[38] However, the well depths and their derivative are not uniquely determined since they depend on the extrapolation method. Indeed, Cowley[39] has proposed another set of values. These will also be considered in order to estimate the influence of the well-depth determination on the pair potential. Our calculated values at liquid density, following either Ese and Reissland, or using the Cowley interpolation scheme, are reported in Table I.

Our calculations, which were done for the numerical integration of the principal-value integrals involved in $F_N(q)$, ensure six-digit precision for this quantity. The computed $v(R)$ of liquid aluminum at 940 K and liquid gallium at 303 K are reported in Figs. 1–3. Before discussing the graphs, it is interesting to note that at the melting point the electron-sphere radius r_s is nearly the same for Al and Ga. Therefore the exchange-correlation contribution, which only varies with r_s, is also the same for the two metals. Moreover, as shown by the computations, the depletion hole and especially the effective mass $m_E(k_F)$ are very similar in Al and Ga, although subordinate to the model parameters, e.g., with Ese-Reissland parameters $m_E(k_F)=0.96$ for Al and Ga, and $\rho^* = -0.157$ and -0.140 for Al and Ga, respectively. Therefore, most of the differences between their pair-potential curves come from the physical contents involved in the well depths.

In Figs. 1–3 we can estimate the pair-potential dependence with (i) model parameters, (ii) the exchange-correlation function, and (iii) the depletion hole distribution, and can compare Al and Ga at every stage.

From Fig. 1 we see that the pair potentials of Al are not too sensitive to sets (1) and (2), which correspond, respectively, to the results of Ese and Reissland,[37] and of Shaw,[11] but are calculated at liquid temperature (Cowley's[39] parameters—not considered here—are, in fact, also very close to those of Ese and Reissland). On the other hand, in Ga the A_2 well depth in set (2) is 12% greater than in set (1). The consequence of this is both a noticeable decrease of the hard-core part of the pair potential, and a decrease of its first minimum by 2.10^{-3} a.u. Compared to the ionic kinetic energy, which is about $k_B T_M \simeq 10^{-3}$ a.u. at the melting point for Ga, this value is not small.

On the graphs in Fig. 2 we note that the VS exchange-correlation scheme produces a deeper pair potential at short range than the IU one whereas the curves are quite similar beyond $R \sim 8$ a.u. The subsiding of the first minimum level is of order $k_B T_M$ in Al, but of order $5k_B T_M$ in Ga. We also note that the IU function gives a repulsive barrier at $R \sim 7$ a.u. which is smaller than $k_B T_M$ in Al, but higher in the case of Ga. Moreover, in the latter case the choice of set (1) combined with the IU scheme yields no minimum in the pair potential in the proximity of the first neighbor.

Figure 3 indicates that the influence of the depletion

TABLE I. Input data for the calculations: well-depth values and first derivative in the liquid state. Set (1) may be compared with the solid calculations of Ese and Reissland (Ref. 37), and set (2) with Cowley's Table III for Ga (Ref. 39) and Shaw's Table II, for Al (Ref. 11).

Set	A_0	$-\partial A_0/\partial E$	A_1	$-\partial A_1/\partial E$	A_2	$\partial A_2/\partial E$
			Al ($T=940$ K, $\Omega=126.7$)			
(1)	1.458	0.266	1.657	0.049		
(2)	1.423	0.325	1.653	0.055		
			Ga ($T=303$ K, $\Omega=128.2$)			
(1)	1.612	0.297	1.843	0.215	1.359	−0.186
(2)	1.601	0.386	1.854	0.220	1.522	0.015

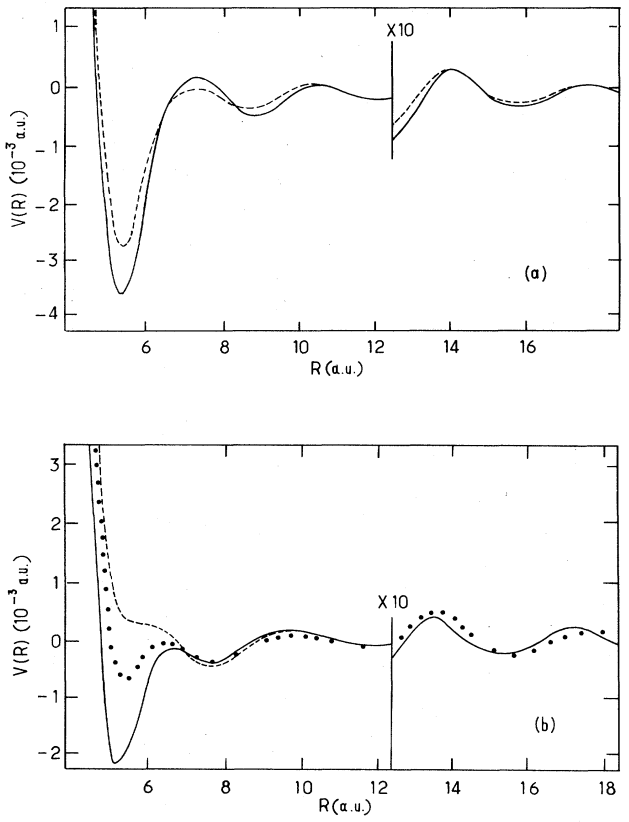

FIG. 1. Pair potentials of (a) liquid Al and (b) Ga. Dependence on model parametrization. According to the legend of Table II, we denote the following: — — —, OMP(1)-VS-UNIF; ——, OMP(2)-VS-UNIF; ●, empirical potential used for MC computation.

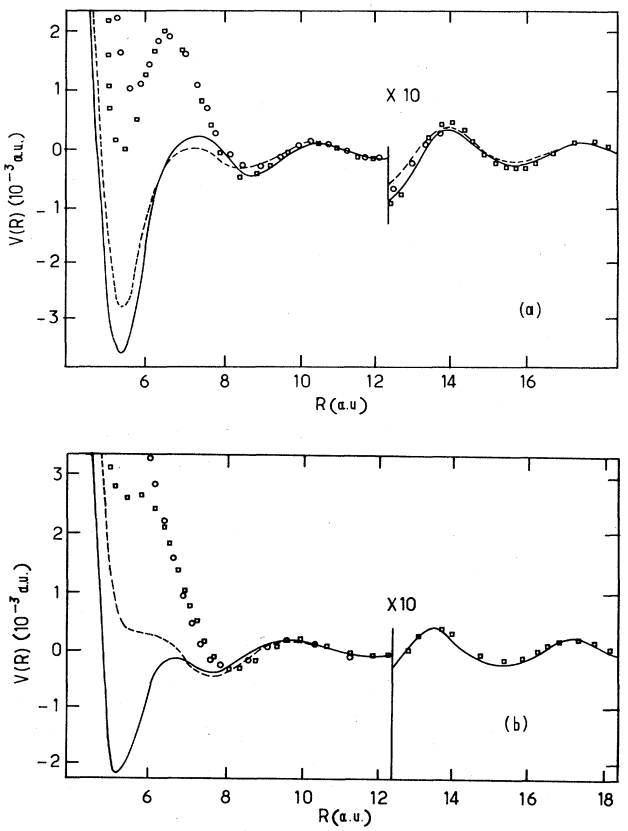

FIG. 2. Pair potentials of (a) liquid Al and (b) Ga. Dependence of screening-function form. According to the legend of Table II, we denote the following: — — —, OMP(1)-VS-UNIF; ——, OMP(2)-VS-UNIF; ○, OMP(1)-IU-UNIF; □, OMP(2)-IU-UNIF.

hole spatial distribution is small compared to the previous factors. We must point out that, in earlier work on aluminum, Rao[40] found that the depletion hole had a stronger influence on the pair potential. In fact, this was observed because the depletion hole charge was allowed to extend beyond the model-radius distance.

Finally, the present section shows that the standard pseudopotential theory generates one class of pair potentials almost identical at long range, whereas at short range some uncertainties remain, mainly due either to optimized model parametrization or local-field exchange-correlation functions. The purpose of the following sections is to discuss the influence of these uncertainties on quantities such as the liquid structure factor or the long-wavelength limit. Before doing that we must analyze how good the connection of $v(R)$ to $S(q)$ by means of the ORPA is.

IV. ORPA OF THE LIQUID METAL STRUCTURE FACTOR

The development of the so-called optimized random-phase approximation (ORPA) has been pioneered by Andersen *et al.*[41,42] and applied to Lennard-Jones fluids. Basically, in this method the pair potential $v(R)$ is separated into a short-range, $v_0(R)$, and long-range part, $v_1(R)$. The former corresponds to the short-range repulsive forces which are at distances smaller than the first minimum position R_0 of the pair potential. The latter contribution is considered a perturbation of $v_0(R)$. In the liquid metal, $v_0(R)$ is assumed to be sufficiently soft to also be subject to perturbation expansion from the hard-sphere reference fluid. This is generally done by means of the "blip-function expansion" of Weeks *et al.*[25] In fact, the ORPA procedure corresponds to the treatment of the hard-sphere model with the perturbation $v_1(R)$ and softness corrections which are optimized in order to keep the pair-correlation function $g(R)$ close to zero inside the core. If we neglect the perturbation $v_1(R)$ in the previous process, we obtain the soft-sphere model, whereas if we describe the hard-sphere reference model with the Percus-Yevick (PY) approach and neglect the soft-sphere correction, we end up with the equivalent of the mean spherical approximation[43] (MSA).

Here, in order to describe the hard-sphere system, we choose a better form than the PY approach, using both the Verlet-Weis[44] and Henderson-Grundke[45] analytical schemes. Moreover, we prefer the diagrammatic expansion of Jacobs and Andersen[15] to the form of Anderson *et al.*[41] because a better low-q $S(q)$ behavior is obtained. [This corresponds to an extension of the blip-function expansion of Jacobs and Andersen,[15] whose validity for po-

lyvalent metals is tested by the direct MC computation (Fig. 6).] A detailed analysis and practical use of the ORPA may be found in several recent works.[46–48,8]

Our main concern here is the structure factor, which, in the ORPA, is readily expressed by

$$S(q)=\frac{1}{1-\rho C_\sigma(q)+\rho[u(q)/k_BT]-\rho B(q)} . \tag{18}$$

ρ is the number density and $C_\sigma(q)$ is the direct correlation function of the hard-sphere system whose diameter σ remains to be chosen. (In the original paper of Andersen *et al.*,[41] the structure factor in place of our relation (18) is expressed by $S(q)=[1-\rho C_\sigma(q)+\rho u(q)/k_BT]^{-1}+\rho B(q)$.)

The term $u(q)$ is the Fourier transform of the optimized potential $u(R)$, namely

$$u(R)=\begin{cases} v(R_0)+k_1+k_2(R/\sigma-1)+(R/\sigma-1)^2\sum_{i=3}^{n} k_iP_{i-3}(2R/\sigma-1), & R<\sigma \\ v(R_0), & \sigma<R<R_0 \\ v(R), & R_0<R \end{cases} \tag{19}$$

where $P_i(x)$ is a Legendre polynomial. The perturbation inside the hard core is generally a smooth continuation of $v(R)$, outside of which the parameters k_i are determined by minimizing the free energy. This optimization condition—which ensures at one and the same time the cancellation of $g(R)$ inside the core—is obtained by solving the system of equations

$$\int q^2\frac{\partial u(q)}{\partial k_i}[S(q,k_i)-S_\sigma(q)]dq=0 . \tag{20}$$

$S_\sigma(q)=[1-\rho C_\sigma(q)]^{-1}$ is the hard-sphere structure factor and $S(q,k_i)$ is the structure factor given by (18) without the quantity $\rho B(q)$.

$B(q)$ is the Fourier transform of the blip function defined in the usual manner by Andersen *et al.*[41] In fact, this approach of the blip function is somewhat different than the approach of Weeks *et al.*[25] because the hard-sphere reference system is replaced by the so-called trial system, defined as

$$w_T(R)=\begin{cases} \infty, & R<\sigma \\ v(R_0), & \sigma<R<R_0 \\ v(R), & R>R_0 . \end{cases}$$

Thus the present blip function is

$$B(R)=y_T(R)\{\exp[-v(R)/k_BT]-\exp[-w_T(R)/k_BT]\} , \tag{21}$$

where $v(R)$ is the actual pair potential and $y_T(R)=g_T(R)\exp[w_T(R)/k_BT]$. Computations involving the present blip function require detailed information about the pair-correlation function $g_T(R)$ of the trial system. The result is that $g_T(R)$ can be easily calculated if $R>\sigma$. On the other hand, when $R<\sigma$, we again need $y_T(R)$ for values of R close to σ only. For this, we use the hard-sphere development[45] of $y_\sigma(R)$ and extrapolate the difference $y_T(R)-y_\sigma(R)$ inside the core using the fact that $y_T(R)$ and its first derivative are continuous functions of R.

Presently, all these quantities are calculated for an arbitrary σ whose optimal value will be self-consistently determined with (20) and the blip-function condition[41]

$$B(q=0)=0 . \tag{22}$$

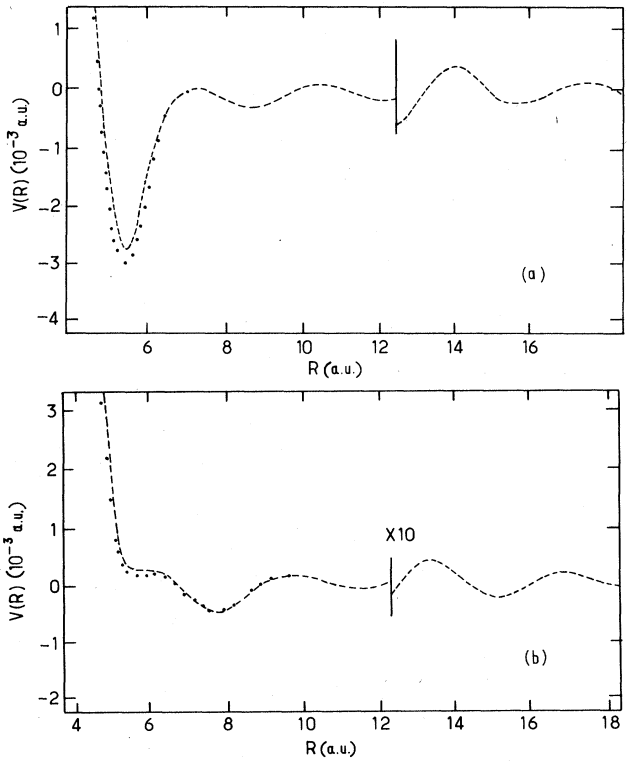

FIG. 3. Pair potentials of (a) liquid Al and (b) Ga. Dependence on the depletion hole distribution. According the legend of Table II, we denote the following: — — —, OMP(1)-VS-UNIF; ●, OMP(1)-VS-EXP.

The latter shows, in fact, that the thermodynamic properties of the actual system at a particular temperature and density are similar to those of the trial system of diameter σ at the same temperature and density. In practice, we calculate the optimal set (k_i,σ) by solving the nonlinear equation system (20) and the condition (22) with a standard Newton procedure.

The only unknown is the number, n, of series terms to be used. Kahl and Hafner[8] have recently demonstrated that, for a wide class of square-well potentials, $n=4$ or 5 is particularly satisfying. We have also systematically investigated this point for the class of oscillatory pair potentials involved here. Figure 4 illustrates, for instance, the $g(R)$ of liquid aluminum with the pair potential of Fig. 1(b) labeled with a dashed line. Clearly, no parameter or one parameter leads to the strong, unrealistic value of $g(R)$ inside the core. On the other hand, a good convergence of $g(R)$ to zero inside the core is obtained with $n=4$. In the case of liquid gallium, its low temperature yields great $u(R)/k_BT$ values, and $n=5$ is a somewhat better choice. Figure 4(b) gives the corresponding structure factor of liquid aluminum up to five parameters. It is clear that a simple RPA or even a one-parameter ORPA are not correct in the main peak region. As we can see in Fig. 4(c), deviations subsist equally in the low-q region. Indeed, with the RPA we find $S(0)=0.0248$, whereas we obtain $S(0)\simeq 0.029$ with the ORPA at $n>2$. This is not at all negligible in view of a comparison between the low-q limit $S(0)$ and the compressibility result, which is 0.017 for Al.

However, before comparing experiment and theory we must emphasize three following points which make an unambiguous interpretation difficult: (i) the accuracy of the structure factor and $S(0)$ data, (ii) the accuracy of the interionic interaction in the model-potential approach through the choice of exchange and correlation, the depletion hole, and the well depths, and (iii) the accuracy of the particular perturbation technique employed to derive $S(q)$ from the given $v(R)$.

Point (i) may be illustrated from the three selected values of x-ray[10] and neutron[49,50] diffraction data of Al. The corresponding graphs in Fig. 5(a) only agree for the position of the peaks, while the amplitude depends on the measurement and normalization procedure. Thus an objective comparison of theory versus experiment for Al would mainly concern the nodes of $S(q)-1$. On the other hand, in the case of Ga the data for x rays[51] and neutrons[52] coincides well [Fig. 5(b)], and this gives us more confidence in the comparison between theory and experiment for Ga.

Regarding point (ii), in our calculations of Al and Ga structure factors we assume that the interionic forces can be modeled by the density-dependent pair potential. This is obtained from model-potential theory, which is taken to be quite adequate for the simple metals. In fact, we must keep in mind that a pair-interaction model does not contain the entire story of the liquid structure since higher-order forces are explicitly involved here. These forces only enter through the assumption that the volume at which we calculate the pair potential is the observed one. Indeed, the important question that arises is whether the

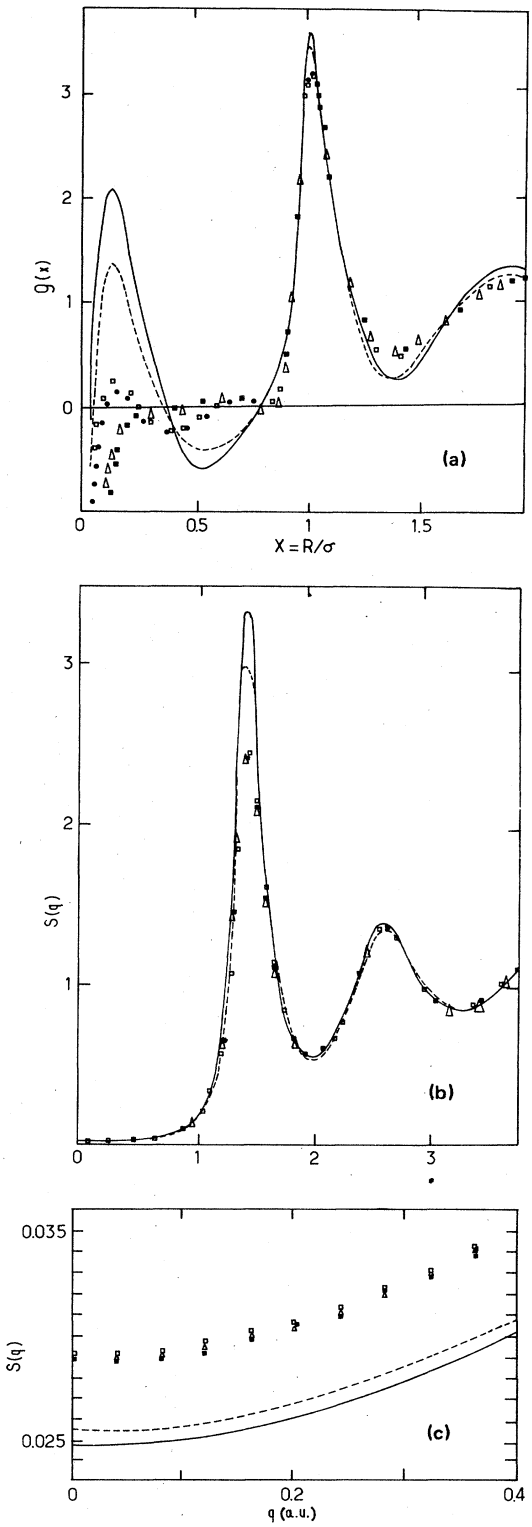

FIG. 4. Influence in the ORPA of the number, n, of series terms in the pair-potential expansion inside the core. The calculations are carried out for Al, with the pair potential corresponding to OMP(1)-VS-UNIF. (a) Pair-correlation function, (b) structure factor, and (c) low-q structure factor. ——, $n=0$ (RPA); — — —, $n=1$; □, $n=2$; ●, $n=3$; △, $n=4$; ■, $n=5$.

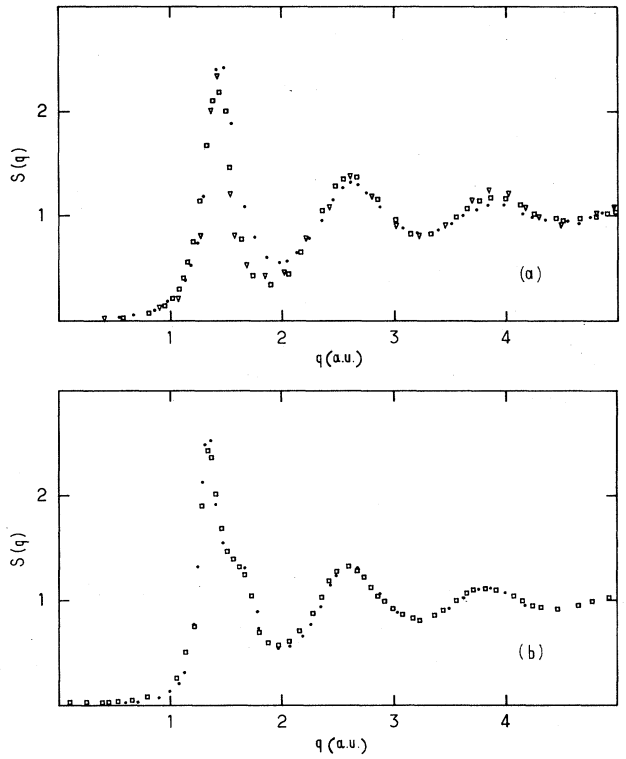

FIG. 5. Experimental data of the structure factor at the melting point. (a) For Al: ●, x-ray diffraction (Ref. 10); □, neutron diffraction (Ref. 49); ▽, neutron diffraction (Ref. 50). (b) For Ga: □, x-ray diffraction (Ref. 51); ●, neutron diffraction (Ref. 52).

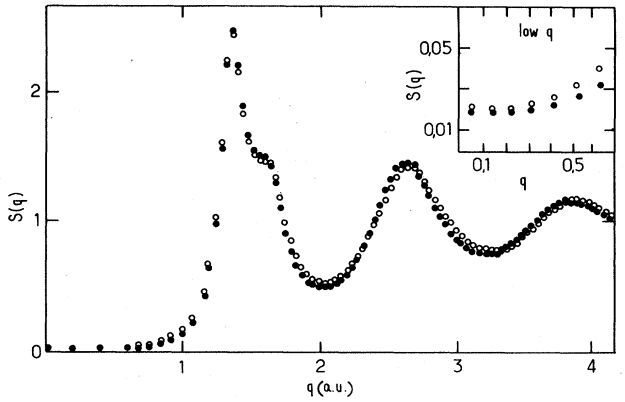

FIG. 6. Gallium structure factor. Comparison between the ORPA and simulation. ○, MC computation; ●, ORPA. The calculations are carried out with the empirical pair potential displayed in Fig. 1(b).

interaction of a pair of ions is slightly altered or disturbed by the variation of many-body forces with the distance and structure. For instance, the existence of a long-range three-body interaction should be treated in third-order perturbation theory, as pointed out by Hasegawa.[53] Fortunately, the degree of success achieved in our calculations suggest that, at least in Al, such many-body effects on structure are small.

We now present a comparison between the ORPA and computer experiment. A useful investigation of point (iii) above can be performed if we dispose of some "exact results" from computer experiments based on the same realistic pair potential, as a reference against which the perturbation method could be tested. We have therefore compared the ORPA with simulations[47] using one of the pair potentials of Ga displayed in Fig. 1(b). As will be seen later, the test for this metal is more instructive than that for Al since the low melting point of Ga implies a stronger effect of the pair-potential oscillations on the structure factor. In Fig. 6 we compare the structure factors from the ORPA and Monte Carlo computation involving a sample of 856 particles. In both cases the pair potential has been truncated at a node near 4σ ($\sigma \sim 5$ a.u.). The MC and ORPA results are equally good since the difference between them falls in the accurate range of the MC method. It should be noted that three sources of error may appear in the MC calculations. One comes from the fit of the potential data. The other two are the statistical errors due to use of a finite number of particles and chains of finite length. Although computer simulations are not well suited to the study of the low-q-limit region, good agreement is found up to the low-q limit, as shown in the inset of Fig. 6. The comparison between the "exact" and less-involved perturbation techniques, such as the RPA or soft-sphere method, clearly demonstrate the superiority of the ORPA (see Fig. 7). We also comment that, in the context of simple polyvalent liquid metals such as Al and Ga, we find that the assumed $S(q)$ expansion by formula (18) agrees better with exact calculation than the original development of Andersen *et al.*[41] Therefore, in the next section we turn to a simultaneous examination of $v(R)$ and $S(q)$ with different local-field exchange-correlation functions, depletion hole distributions, and well depths of the model potential.

V. STRUCTURE FACTORS FROM THE PSEUDOPOTENTIAL APPROACH: RESULTS AND DISCUSSION

The main aim of the present investigation is to compare the calculated structure factors with experiment while analyzing the influence of (i) the $v(R)$ different parts by means of the ORPA and the soft-sphere approximation, and (ii) the model-potential ingredients. Although there is no proper treatment for the structure factor at high and low q, we shall discuss the results separately for the sake of simplicity.

A. Global analysis of $S(q)$

At first glance, Table II indicates that all the aluminum pair potentials have a similar core diameter σ. We find that the variation of the packing fraction η among the various models lies between 0.471 and 0.484. In turn, the spread of η is more pronounced in Ga (0.459—0.545) than in Al, although all the values are reasonable. In terms of the hard-core diameter, this means that we expect the mean distance in liquid Ga to lie between 4.82 and 5.11

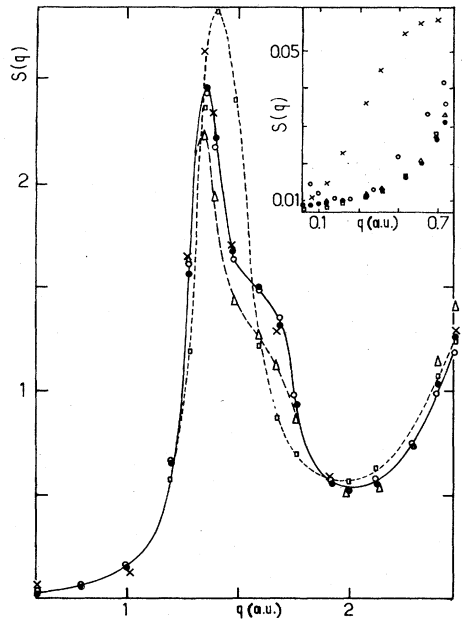

FIG. 7. Gallium structure factor. Comparison between different approximations. □, soft-sphere approximation (JA); △, RPA; ●, ORPA with the JA approximation; ×, ORPA with the WCA approximation; ○, MC computation. The calculations are carried out with the empirical pair potential displayed in Fig. 1(b).

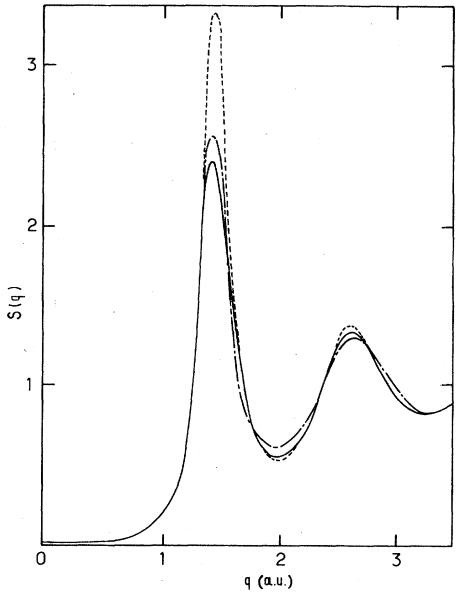

FIG. 8. Aluminum structure factor. Comparison between different approximations. —·—·—, soft-sphere approximation; — — —, RPA; ——, ORPA with $n=5$. The calculations are carried out with the pair potential issued from the OMP(1)-VS-UNIF model potential.

a.u., in good accordance with structural data. This ensures that the core part of the pair potentials generated by various models is sufficiently realistic in order to carry out the perturbation expansion.

In addition, Fig. 8 shows the differences between structure factors obtained with the soft-sphere approximation, labeled JA,[15] where JA represents Jacob and Andersen, and the ORPA. Thus, with the attractions and Friedel's oscillations, the first peak of the aluminum $S(q)$ tends to become flatter and broader, whereas the high-q oscillations are slightly accentuated and contracted. It is worth noting that if these discrepancies remain small the same inference is reached whatever the chosen pair potentials. Our calculations are quite similar for gallium (Fig. 7), but the effects of the Friedel oscillations are much more marked, e.g., the attenuation in the height of the main peak of $S(q)$ and the appearance of a shoulder on it. These results are in partial agreement with the observations of Jacobs and Andersen,[15] which shows that the longer-range attractions affect the height but not the position of the principal peak. One possible explanation of the behavior of Al and Ga can be provided by the $S(q)$ temperature dependence. At high T the factor $1/k_BT$ which binds $v(R)$ and $c(R)$ mostly reduces the influence of the long-range part of $v(R)$. For Ga, having a low melting point, the presence of the Friedel oscillations drastically affects the main peak of $S(q)$, but for Al, which has a relatively high melting temperature, the ion kinetic energy is sufficiently large to overcome the potential barriers, and therefore the liquid structure is much less sensitive to the Friedel oscillations. From these remarks we realize why the use of a simple local pseudopotential such as that of Ashcroft by McLaughlin and Young[7] works well for the Al liquid structure, once the parameter R_c has been adjusted in order to define a reasonable packing fraction.

Now we can afford to give a substantial answer to the question concerning the factors of the pair potential which are most influential in determining the form of $S(q)$. A recrudescence of activity in this subject seems to indicate a preference for the short-core part, whereas a limited role is reserved for the Friedel oscillations.[54,55] Without a doubt, for "soft" systems such as Na or Rb governed by a R^{-4} potential[56] it is the soft part of the potential which mainly determines the structure. However, for a polyvalent liquid metal such as Ga and, to a lesser extent, Al, the Friedel oscillations have a special influence, principally marked on the main peak of $S(q)$. Otherwise, as will be seen later, the interactions in the near-neighbor region lead to the principal departure from the hard-sphere structure behavior in the low-q region. Recently, this has been also noted by Dharma-wardana and Aers,[57] who found that the behavior of the potential at the first-neighbor position is essential in order to derive a precise value of $S(0)$ of liquid Al.

B. Sensitivity of $S(q)$ to input data

We now consider, in greater detail, the change of $S(q)$ from one pair potential to another on the basis of the model-potential ingredients. Inspection of Figs. 9 and 10 indicates that the aluminum structure factor is neither very sensitive to the choice of model-potential well depths nor to the particular exchange-correlation function con-

TABLE II. Values of $S(0)$ in the JA, RPA, and ORPA schemes for the class of pair potentials displayed in Figs. 1 and 2. OMP is the optimized model potential of Shaw with constant effective mass included. OMP(1) and OMP(2) correspond to the choice of well depth of Table I; VS and IU are the screening functions of Vashishta and Singwi (Ref. 34) and Ichimaru and Utsumi (Ref. 35), respectively. UNIF and EXP denote, respectively, the uniform and exponential depletion hole distributions.

Model	η	$[S(0)]_{JA}$	$[S(0)]_{RPA}$	$[S(0)]_{ORPA}$	$\{S(0)-[S(0)]_{expt}\}/k_BT$	$[S(0)]_{expt}$
			Al (T=940 K)			
OMP(1)-VS-UNIF	0.482	0.0215	0.0252	0.0291	4	
OMP(1)-VS-EXP	0.471	0.0237	0.0289	0.0340	5.7	
OMP(1)-IU-UNIF	0.484	0.0212	0.0191	0.0203	1.1	0.017[a] or 0.20[b]
OMP(2)-VS-UNIF	0.473	0.0234	0.0295	0.0372	6.7	
OMP(2)-IU-UNIF	0.471	0.0238	0.0221	0.0251	2.7	
			Ga (T=303 K)			
OMP(1)-VS-UNIF	0.545	0.0122	0.0123	0.0106	6	
OMP(1)-VS-EXP	0.524	0.0147	0.0151	0.0131	8.6	
OMP(2)-VS-UNIF	0.459	0.0263	0.0453	0.0625	60	0.0048[c] or 0.010[b]
OMP(2)-IU-UNIF	0.473	0.0234	0.0148	0.0127	8.2	
Empirical	0.505	0.0174	0.0185	0.0182	13.9	

[a]Reference 58.
[b]Reference 10.
[c]Reference 61.

sidered here. Firstly, the discrepancy due to these local-field functions—which is exhibited on the top of the main peak (Fig. 9)—is connected neither to the short- nor long-range interactions, but mainly to the intermediate-range interactions. This is clearly illustrated by the two pair potentials [Fig. 2(a)] which have identical oscillations beyond 8 a.u. and a very similar hard core corresponding to the packing fractions 0.482 and 0.484. This last point is not evident on Fig. 2(a), but we must keep in mind that η is obtained by using the blip-function method. Incidentally, this means that the present exchange-correlation choice is not an important factor in the derivation of the interactions at short and long range and the description of the general form of $S(q)$ for Al. Similar conclusions were reached by Dharma-wardana and Aers[57] and Hayter *et al.*[54] The former found that the behavior of the large-R pair potential in Al is not very sensitive to the local field, while the latter noted the possibility of reproducing $S(q)$ by using the simple classical Thomas-Fermi screening, at least in the cases of Na, K, and Rb.

It is interesting to note that the change of the well-depth values from OMP(1) to OMP(2) (Table I) (OMP denotes optimized model potential) leads to a small variation in the two first peaks of $S(q)$. More precisely, OMP(1) gives a packing fraction slightly greater than OMP(2) (0.482 versus 0.473, respectively) and a small shifting of the Friedel oscillations [Fig. 2(a)]. All these contribute to affect $S(q)$. We observe that, in OMP(1), A_0 is greater than in OMP(2), whereas the A_1 parameters are very similar in each case. Therefore, considering optimization condition (3), the model radius R_0 of OMP(1) is smaller than that of OMP(2). However, as previously seen, $\eta_1 > \eta_2$, so that $\sigma_1 > \sigma_2$. According to this result, we note that an increase of the model radius does not necessarily imply an increase of the core diameter σ. This feature is certainly not incorrect, since there is a delicate redistribution between both direct and indirect interaction energies giving the pair potential, through all the ingredients involved in the theory.

It is again of interest to mention that, by considering different spatial distributions of the depletion hole with the total charge criteria adopted here, we found the effect on $S(q)$ to be small. Moreover, the pair potential, obtained here from the model-potential scheme, includes additional effective-mass contributions which largely influence the short-range part of the pair potential. It is important to point out that without these contributions the structure factor of Al is less reliable to experiment (Fig. 11).

For Ga the study of the influence of the various input data is more complicated. Contrary to Al, regarding the exchange-correlation effects, the choice of the local-field functions becomes crucial because it can drastically modify the profile of the main peak of $S(q)$. It is desirable to consider simultaneously the pair potentials of Fig. 2(b)

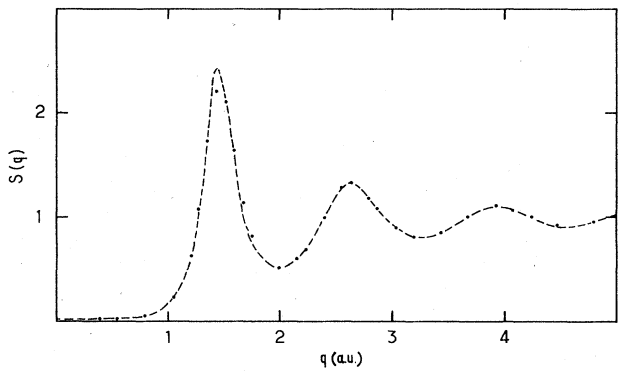

FIG. 9. Aluminum structure factor. Influence of the different screening functions. — — —, OMP(1)-VS-UNIF; ●, OMP(1)-IU-UNIF.

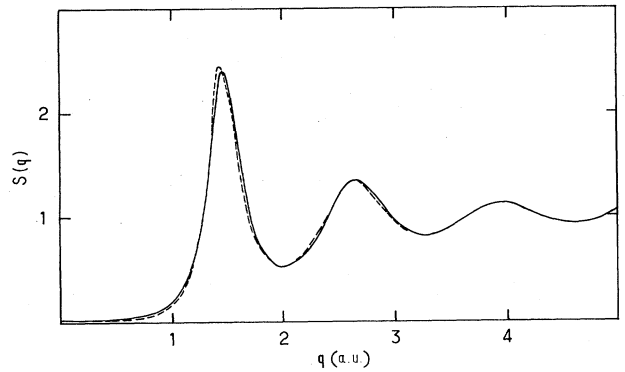

FIG. 10. Aluminum structure factor. Influence of the different well-depth values. — — —, OMP(1)-VS-UMF; ——, OMP(2)-VS-UNIF.

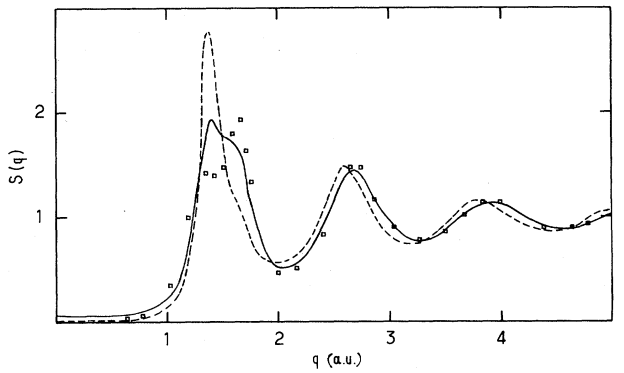

FIG. 12. Gallium structure factor. Influence of different screening functions and well-depth values. — — —, OMP(1)-VS-UNIF; ——, OMP(2)-VS-UNIF; □, OMP(2)-IU-UNIF.

and the corresponding $S(q)$ (Fig. 12). As for Al, the pair potentials [OMP(2)-VS] and [OMP(2)-IU] are very close to each other beyond 10 a.u. Therefore, this indicates that the difference in the exchange-correlation functions does not affect the long-range interactions in Ga. Thus the strong change which is observed in the splitting of the principal peak of $S(q)$ (Fig. 12) does not come from a modification in these long-range interactions, although this does not necessarily mean that they do not manifest themselves clearly in $S(q)$. Besides, if we characterize the short-range interactions of the two pair potentials by the packing fraction η, the difference between them is only 0.015. Such a change alone is not sufficient to explain quantitatively the variation in the $S(q)$ profile. Therefore, in the case of gallium a precise exchange-correlation determination is required as is a good estimation of the pair potential in the first-neighbor region. Contrary to Al, the intermediate region and Friedel oscillations are of central importance for Ga structure.

We now turn to the problem of the well-depth determination in Ga. The two sets of s and p wells evaluated in the liquid state are very close to each other (Table I). The A_l are assumed to vary linearly over the occupied band, but the slope $\partial A/\partial E$ can drastically change, mainly for A_2. This is attributed to the difficulty in defining the derivation of the curve $A_l(E)$ specified by only two or three points. Thus, inspection of Fig. 12 shows that the biggest change in $S(q)$ is due to the term A_2. Indeed, the large value of the packing fraction ($\eta=0.545$) for the reference hard-sphere system, corresponding to the shallower d well, contributes to the increase of the height of the first peak, but a sensible tightening of the other oscillations is observed. Finally, we can appreciate, without comment, in Fig. 13, the small effect of the depletion hole distributions, confirming the previous results on Al.

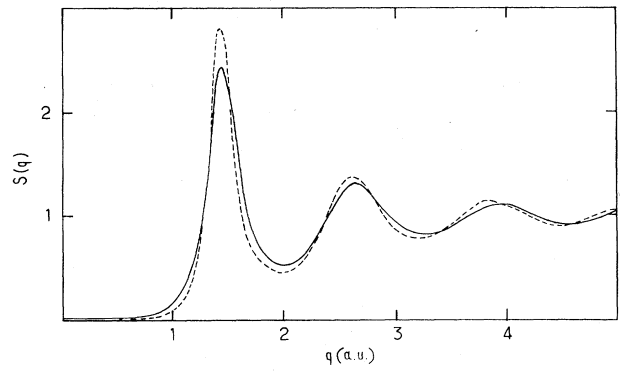

FIG. 11. Aluminum structure factor. Influence of the constant effective mass $m_E(k_F)$. ——, with $m_E(k_F)$; — — —, without $m_E(k_F)$. The calculations are carried out with the pair potential issued from the OMP(1)-VS-UNIF model potential.

C. Low-q behavior and $S(0)$ calculation

Accurate experiments at low wave number are difficult. However, special measurements have been reported by Waseda. For instance, it is interesting to note that $S(0)$'s extrapolation procedure gives, for Al, $S(0)=0.0186$. This value is very close to the $S(0)$ derivation from compressibility[58] (0.017). In the case of Ga the measurements are increasingly difficult since the $S(0)$ value is 3 times smaller than that in Al. Narten[52] has supplied low-q values of $S(q)$ which are extrapolated to obtain the compressibility result for $S(0)$ at 296 K [$S(0)=0.0048$]. On the other hand, the smooth extrapolation of Bizid *et al.*[51] does not assume the isothermal compressibility result, and they indicate $S(0)\simeq 0.011$ at 323 K.

It is useful to note that, at melting point, liquid-Al and Ga compressibilities [$\chi_T=S(0)/\rho k_B T$] are nearly equal [$\chi_T(\mathrm{Al})\simeq 1.1\chi_T(\mathrm{Ga})$]. Moreover, as we have previously pointed out, the number density ρ of liquid Al and Ga is the same at melting, so that $S(0)/T$ is almost identical for the two metals. For this reason we express the difference between theory and experiment in terms of $\{[S(0)]_{\mathrm{theor}}-[S(0)]_{\mathrm{exp}}\}/k_B T$ in the last column of Table II. The theoretical result is labeled $[S(0)]_{\mathrm{ORPA}}$, but we also report (in Table II) the intermediate result, which corresponds to the neglect of the explicit influence of the long-range part. This soft-sphere approximation is labeled $[S(0)]_{\mathrm{JA}}$. In addition, the result labeled $[S(0)]_{\mathrm{RPA}}$ is obtained if we set the optimized contribution of the pair potential equal to zero inside the core.

As we have already noted for Al, the hard-core

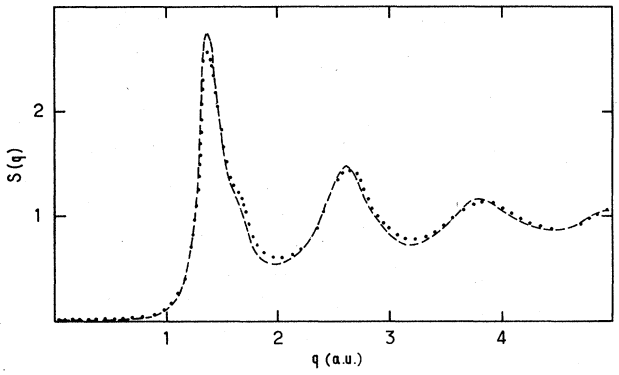

FIG. 13. Gallium structure factor. Influence of different depletion hole distributions. — — —, OMP(1)-VS-UNIF; ●, OMP(1)-VS-EXP.

reference-system diameters associated with the various pair potentials investigated here are quite similar in all cases. Consequently, the $[S(0)]_{JA}$ values due to the repulsive short-range part are almost the same whatever the model, lying between 0.0212 and 0.0238. On the contrary, the long-range part of the pair potential associated with the screening may have a stronger influence. For instance, considering OMP(1) parameters and a uniform depletion hole, with VS screening, we find $[S(0)]_{ORPA}=0.0291$, while with IU screening we obtain $[S(0)]_{ORPA}=0.0203$. Generally, our results with the VS local field rather disagree with the experimental results. Nevertheless, it is difficult to draw a definite conclusion for this because other factors may have been omitted in the local-field $G(q)$ which might reverse the statement. However, it may be, in the present context, that a high value of $S(0)$ corresponds to the VS local field, while a lower value of $S(0)$ is favored by the IU local field. This fact has also been pointed out by Dharma-wardana and Aers.[57]

We can again see from Table II that the $S(0)$ value is also very sensitive to the well-depth choice as well as the depletion hole distribution.

For Ga we have encountered difficulties in order to obtain a convenient quantitative agreement for the main peak of the structure factor, because it appears to be very much more sensitive to the ingredients of pseudopotential theory than in the case of Al. Clearly, this is also true for the low-q region. We note that the effects of the short- and long-range parts of the pair potential on $S(0)$ vary from one model to another.

The influence of the exchange-correlation scheme is important in several ways. Thus if we only consider the short-range part of the pair potential, we find no physical packing fraction for the OMP(1)-IU scheme, while with the OMP(1)-VS scheme we obtain $\eta=0.545$. With the second set of well-depth values, the difference between the VS and IU schemes is not very pronounced, since $\eta=0.459$ and 0.473, respectively. On the other hand, considerable differences come from the long-range part of the pair potentials since we obtain $[S(0)]_{ORPA}=0.0625$ from OMP(2)-VS and 0.0127 from OMP(2)-IU.

Concerning the well depths, the contribution of d electrons to the pseudopotential is an important factor in Ga, and the lack of a unique way in the estimation of A_2 and $\partial A_2/\partial E$ leads to considerable incertitude in the liquid-structure-factor theoretical derivation. In turn, the experimental $S(q)$ may be regarded as a guide to fit the gallium pseudopotential through A_2. Here we find that, with OMP(2), $S(q)$ disagrees with experiment in the main-peak and low-q regions if the VS local field is used. The high value of $[S(0)]_{ORPA}=0.062$ occurs because the attractive well of the pair potential at the first-neighbor distance is too deep compared to k_BT [Fig. 2(b)] and therefore the atoms are extremely trapped in it. If we consider the OMP(2)-IU scheme, we find a value of $[S(0)]_{ORPA}=0.0127$, which is close to the extrapolation of Bizid *et al.*,[51] but disagrees with the compressibility result, as well as with the main peak, as previously demonstrated. The pair potential which issues from OMP(2)-IU, contrary to OMP(2)-VS, has a repulsive barrier at the near-neighbor distance which is greater than k_BT. Its effect reduces the value of $S(0)$ from 0.0234 to 0.0127, but at the same time removes the atoms from the hard-sphere structure, causing the main peak of $S(q)$ to be greatly distorted.

Finally, if we focus on the OMP(1)-VS-UNIF (UNIF denotes uniform) scheme we obtain a good accordance—both in the main-peak and low-q regions—with the data of Bizid *et al.*[51] This shows that within standard pseudopotential theory a fine determination of the well-depth values may lead to a fair agreement. There is no reason to invoke more complex interionic forces than those of the present model to reproduced the observed $S(q)$. It is worth mentioning that the pair potential corresponding to OMP(1)-VS-UNIF is moderately perturbed from the hard-sphere potential, e.g., there is a small repulsive ledge of $0.25k_BT$ between 5 and 7 a.u., and a Friedel oscillatory behavior in the long-range part. However, $S(q)$ is rather well reproduced, on the whole as well as its singularities, indicating, in fact, that the shoulder in the main peak can be associated with small pair-interaction forces.

VI. CONCLUSION

We have attempted to emphasize the link between the liquid-metal structure and the interactions arising from its two-component electrons and ions by means of the standard simple-metal pseudopotential formalism. Much work has been done on this subject over the least decade. Here the improvements come from the association of the rigorous nonlocal model-potential theory of Shaw with an accurate analytical derivation of the structure factor by the ORPA. Our choice of Shaw's model for the electron-ion interaction has been guided by the fact that it is fully determined from atomic data, without any arbitrary adjustment, and because its wide use in the literature has confirmed its applicability to many electronic and ionic properties, such as the density of states, phonon spectra, interatomic forces, and the constant stability of crystalline phases.

To improve the structure-factor derivation we have taken into account the long-range oscillatory nature of the metal potential through the ORPA, and we have shown by comparison with Monte Carlo computations the limi-

tation of particular thermodynamic perturbation methods such as the RPA or the soft-sphere model. On that point, we conclude that the ORPA substantially improves the $S(q)$ derivation, giving accurate values at all wave numbers. Moreover, since very moderate computation time is required in the ORPA program, many pair potentials have been tested.

Thus we have been able to point out the principal factors of the pseudopotential theory that most influence the liquid structure, and to clarify the striking differences between aluminum and gallium. Our work shows that to go beyond the classical soft-sphere analysis of $S(q)$, one needs an accurate derivation of two basic quantities, namely the bare electron-ion pseudopotential and the local-field exchange-correlation function. However, the case of Shaw's model, effective masses and depletion hole distribution may also have some importance, depending on the particular metal under study. However, we think that most of the difficulties in obtaining a quantitative agreement for the liquid Ga structure are due to its too low melting temperature, which necessitates a more precise derivation of the electron-ion interaction, whereas the electron-electron interaction is certainly less important. Although Al and Ga have a very similar electronic density, the diffraction information on the atomic arrangement assumes that no structural anomalies are observed in the Al structure, while the salient features of Ga structure are a shoulder on the main peak of $S(q)$ and a low $S(0)$. In the context of the linear-response theory, the electron-gas response function depends only on its density; thus it seems unlikely that these anomalies are caused by the electron gas.

Finally, in order to improve the situation of low-melting-point metals such as Ga and probably Hg, we must first search for a better *ab initio* determination of the electron-ion pseudopotential. Therefore, similar calculations would be fruitfully pursued using basic pseudopotentials such as the new family of energy-independent pseudopotentials introduced by Hamann *et al.*,[59] or the general pseudopotential theory of Moriarty,[60] which takes advantage of the orthogonalized-plane-wave approach.

[1]N. W. Ashcroft and J. Lekner, Phys. Rev. **145**, 83 (1966).
[2]Y. Waseda, in *Liquid Metals 1976*, edited by R. Evans and D. A. Greenwood (IOP, London, 1977), p. 230.
[3]C. Regnaut, J. P. Badiali, and M. Dupont, J. Phys. (Paris) Colloq. **41**, C8-603 (1980).
[4]H. Beck and R. Oberlé, J. Phys. (Paris) Colloq. **41**, C8-289 (1980).
[5]R. Evans and T. J. Sluckin, J. Phys. C **14**, 3137 (1981).
[6]M. Rami Reddy, L. R. Vijayalaxmi, and K. N. Swamy, Phys. Lett. **82A**, 353 (1981).
[7]I. L. McLaughlin and W. H. Young, J. Phys. F **12**, 245 (1982).
[8]G. Kahl and J. Hafner, Phys. Chem. Liquids **12**, 109 (1982); for an analysis of the trends of the liquid structure with the valency, see J. Hafner, J. Non-Cryst. Solids **61-62**, 175 (1984).
[9]J. L. Bretonnet and C. Regnaut, J. Phys. F **14**, L59 (1984).
[10]Y. Waseda, *The Structure of Non-Crystalline Materials, Liquids and Amorphous Solids* (McGraw-Hill, New York, 1980).
[11]R. W. Shaw, Phys. Rev. **174**, 769 (1968).
[12]R. Kumaravadivel and R. Evans, J. Phys. C **9**, 3877 (1976).
[13]A. J. Greenfield, J. Wellendorf, and N. Wiser, Phys. Rev. A **4**, 1607 (1971).
[14]M. J. Huijben, thesis, Rijksuniversiteit Gröningen, 1978.
[15]R. E. Jacobs and H. C. Andersen, Chem. Phys. **10**, 73 (1975).
[16]R. S. Day, F. Sun, and P. H. Cutler, Phys. Rev. A **19**, 328 (1979).
[17]C. Regnaut, J. P. Badiali, and M. Dupont, Phys. Lett. **74A**, 245 (1979).
[18]R. Oberlé and H. Beck, Solid State Commun. **32**, 5103 (1979).
[19]P. T. Cummings and G. Stell, Mol. Phys. **43**, 1267 (1981).
[20]J. L. Bretonnet, Solid State Commun. **47**, 395 (1983).
[21]M. Silbert and W. H. Young, Phys. Lett. **58A**, 469 (1976).
[22]J. L. Bretonnet, J. G. Gasser, A. Bath, and R. Kleim, Phys Status Solidi B **114**, 243 (1982).
[23]K. K. Mon, N. W. Ashcroft, and G. V. Chester, Phys. Rev. B **19**, 5103 (1979); **22**, 5014(E) (1980).
[24]R. Evans and W. Schirmacher, J. Phys. C **11**, 2437 (1978).
[25]J. D. Weeks, D. Chandler, and H. C. Andersen, J. Chem. Phys. **54**, 5237 (1971).
[26]K. K. Mon, R. Gann, and D. Stroud, Phys. Rev. A **24**, 2145 (1981).
[27]R. L. Henderson and N. W. Ashcroft, Phys. Rev. A **13**, 859 (1976).
[28]M. H. Cohen and V. Heine, Phys. Rev. **122**, 1821 (1961).
[29]W. A. Harrison, *Pseudopotentials in the Theory of Metals* (Benjamin, New York, 1966).
[30]R. W. Shaw, J. Phys. C **2**, 2335 (1969).
[31]R. W. Shaw, J. Phys. C **2**, 2350 (1969).
[32]M. P. D'Evelyn and S. A. Rice, J. Chem. Phys. **78**, 5225 (1983).
[33]R. W. Shaw, J. Phys. C **3**, 1140 (1970).
[34]P. Vashishta and K. S. Singwi, Phys. Rev. B **6**, 875 (1972).
[35]S. Ichimaru and K. Utsumi, Phys. Rev. B **24**, 7385 (1981).
[36]L. E. Ballentine and O. P. Gupta, Can. J. Phys. **49**, 1549 (1971).
[37]O. Ese and J. A. Reissland, J. Phys. F **3**, 2066 (1973).
[38]A. F. Crawley, Int. Met. Rev. **19**, 32 (1974).
[39]F. R. Cowley, Can. J. Phys. **54**, 2348 (1976).
[40]P. V. S. Rao, J. Phys. Chem. Solids **35**, 669 (1974).
[41]H. C. Andersen, D. Chandler, and J. D. Weeks, J. Chem. Phys. **56**, 3812 (1972).
[42]H. C. Andersen, D. Chandler, and J. D. Weeks, Adv. Chem. Phys. **35**, 105 (1976).
[43]J. A. Barker and D. Henderson, Rev. Mod. Phys. **48**, 587 (1976).
[44]L. Verlet and J. J. Weis, Phys. Rev. A **5**, 939 (1972).
[45]D. Henderson and E. W. Grundke, J. Chem. Phys. **63**, 601 (1975).
[46]N. K. Ailawadi, Phys. Rep. **57**, 241 (1980).
[47]C. Regnaut, thèse d'Etat, Université Paris, 1981.
[48]J. L. Bretonnet, thèse d'Etat, Université Metz, 1982.
[49]J. M. Stallard and C. M. Davis, Phys. Rev. B **8**, 368 (1973).
[50]D. Jovic, I. Padureanu, and S. Rapeanu, in *Liquid Metals 1976*, edited by R. Evans and D. A. Greenwood (IOP, Lon-

don, 1977), p. 120.
[51]A. Bizid, L. Bosio, and R. Cortes, J. Chem. Phys. **74**, 863 (1977).
[52]A. H. Narten, J. Chem. Phys. **56**, 1185 (1972).
[53]M. Hasegawa, J. Phys. F **6**, 649 (1976).
[54]J. B. Hayter, R. Pynn, and J. B. Suck, J. Phys. F **13**, L1 (1983).
[55]W. H. Young, A. Meyer, and M. Silbert, J. Non-Cryst. Solids **61-62**, 219 (1984).
[56]J. P. Hansen and D. Schiff, Mol. Phys. **25**, 1281 (1973).
[57]M. W. C. Dharma-wardana and G. C. Aers, Phys. Rev. B **28**, 1701 (1983).
[58]G. M. B. Webber and R. W. B. Stephens, in *Physical Acoustics,* edited by W. P. Mason (Academic, New York, 1968), Vol. IV B, p. 53.
[59]D. R. Hamann, M. Schlüter, and C. Chiang, Phys. Rev. Lett. **43**, 1494 (1979).
[60]J. A. Moriaty, Phys. Rev. B **26**, 1754 (1982).
[61]A. Defrain, J. Chem. Phys. **74**, 851 (1977).